Macromolecules **2005,** *38,* 10185−10191

Structure−Property Study of Diblock Copolymer Micelles: Core and Corona Radius with Varying Composition and Degree of Polymerization

Carlos Guerrero-Sanchez,[†] Daan Wouters,[†] Charles-André Fustin,[‡] Jean-François Gohy,[‡] Bas G. G. Lohmeijer,[†] and Ulrich S. Schubert*,[†]

Laboratory of Macromolecular Chemistry and Nanoscience, Eindhoven University of Technology and Dutch Polymer Institute (DPI), P.O. Box 513, 5600 MB Eindhoven, The Netherlands, and Unité de Chimie des Matériaux Inorganiques et Organiques (CMAT), Département de Chimie, Université catholique de Louvain, Place L. Pasteur 1, B-1348 Louvain-la-Neuve, Belgium

Received July 15, 2005; Revised Manuscript Received September 19, 2005

ABSTRACT: The synthesis and characterization of well-defined poly((styrene-*alt*-diphenylethylene)-*b*-isoprene) diblock copolymers via sequential anionic polymerization are discussed. Indeed, modified 1,1-diphenylethylene commodity elastomers have appeared recently as an alternative to the well-known elastomers for high-temperature applications. The obtained materials were used for the preparation of block copolymer micelles. The hydrodynamic radius of the micelles in solution was determined by dynamic light scattering and the size of the core by atomic force microscopy at dry conditions. It was found that the observed characteristics of the studied micelles correlate to theoretical scaling predictions. Moreover, the average size of the unimers could be determined with high precision from the obtained experimental data and theoretical knowledge.

Introduction

Diblock copolymers are well-known for their abilities to spontaneously assemble into nano-ordered structures. On surfaces and in bulk diblock copolymers with immiscible blocks may phase separate, yielding spherical, cylindrical, and lamellar or gyroidal phase-separated structures depending on the block copolymer composition and architecture. When block copolymers with incompatible blocks are dissolved in a thermodynamically good solvent for one block but a bad solvent for the other block, the copolymer chains associate reversibly to form micelles. Recently, block copolymer micelles received increasing attention because of their possible applications as carriers in drug delivery applications[1] and for the preparation of stabilized nanoparticles.[2] Depending on the block copolymer chain architecture (i.e., cyclic, comb, star) and on the block copolymer composition, not only spherical micelles but also cylinders,[3] rods,[4,5] vesicles,[6] and bilayers[5] can be formed. The preparation of micelles by direct dissolution of a block copolymer in a selective solvent is generally not very suitable due to the poor solubility of bulk block copolymers.[7] Moreover, the characteristic features of the obtained micelles could be then determined by the bulk structure, especially in the case of high-T_g core-forming blocks. To circumvent these drawbacks, the initial dissolution of the bulk block copolymer in a common solvent is often preferred because it allows a complete solubilization of the sample, and it erases memory effects from the starting bulk morphology. A selective solvent for the coronal blocks is then added, followed by removal of the common solvent by stripping or dialysis.[7,8]

The size of the micelles may be determined experimentally[8−10] by light scattering techniques, SANS and SAXS, TEM, size exclusion chromatography, and analytical ultracentrifugation and is known to depend on block copolymer composition, interaction parameter χ_{AB} between the blocks, solvent quality, temperature, and, in the case of block copolymers with ionizable blocks, pH. For both charged and neutral block copolymer systems models have been developed on the basis of mean-field theories,[11,12] Monte Carlo simulations,[13] free energy calculation,[14] and scaling theories.[15]

Systematic studies showing the correlation between block copolymer composition and the hydrodynamic radius of diblock copolymer micelles have been reported, e.g., for poly(ethylene oxide-*b*-caprolactone) in water[16] and poly(styrene-*b*-alkyl methacrylates) in dodecane solutions.[17] In those studies the hydrodynamic radius of micelles was determined by dynamic light scattering (DLS) and has been correlated to different degrees of polymerization and block compositions. The micellar core radius was either estimated from scaling theories or determined using transmission electron microscopy.[17]

For the study presented here, micelles have been prepared from four different diblock copolymers of poly((styrene-*alt*-diphenylethylene)-*b*-isoprene) with varying composition and molecular weights. This system is similar to commodity elastomers (AB and ABA block copolymers where A is polystyrene and B is a polydiene). For some decades the micellization behavior of commodity block copolymers has attracted the attention of scientists.[10] Remarkable differences have been reported for micelles of poly(styrene-*b*-isoprene) block copolymers depending on their macromolecular architecture (i.e., miktoarm stars vs linear diblock copolymers or cyclic vs linear).[18−20] However, to the best of our knowledge, the influence of incorporating different comonomers into these block copolymers has not been investigated. The incorporation of different comonomers into these block copolymers aims mainly at the improvement of their properties. To achieve this chemical modification, “new” synthetic methods have appeared by polymerizing “bulky” monomers in the glassy portion (A) of the blocks, such as α−methylstyrene and 1,1-diphenylethylene.[21−23]

[†] Eindhoven University of Technology and Dutch Polymer Institute (DPI).

[‡] Université catholique de Louvain.

* Corresponding author. E-mail: u.s.schubert@tue.nl.

10.1021/ma051544u CCC: $30.25

Scheme 1. Reaction Scheme for the Synthesis of Poly((styrene-*alt*-1,1-diphenylethylene)-*b*-isoprene) Block Copolymers (Samples 1−4 of Table 1) via Sequential Anionic Polymerization

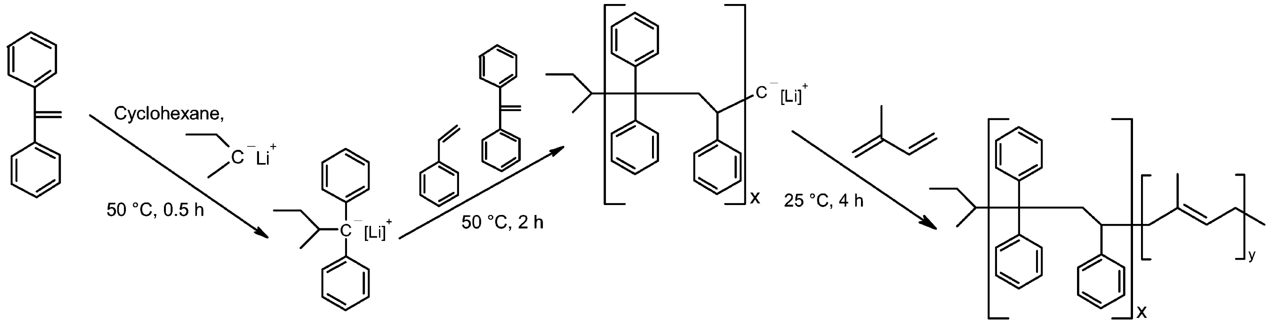

1,1-Diphenylethylene can be copolymerized via anionic polymerization with styrene and diene monomers to lead to an important improvement on the long-term service temperature of polystyrene (glass transition temperature increases up to 170−180 °C, depending on the 1,1-diphenylethylene content).[21−23] Furthermore, it is known from the literature that 1,1-diphenylethylene does not homopolymerize since its monomer reactivity ratio is close to zero. However, when 1,1-diphenylethylene is copolymerized with styrene or dienes, alternating-type copolymers are obtained.[24] Here we discuss the synthesis and micellization behavior of different diblock copolymers of poly((styrene-*alt*-diphenylethylene)-*b*-isoprene). The diblock copolymers were synthesized via sequential anionic polymerization and characterized by means of gel permeation chromatography (GPC), ^{1}H NMR, and differential scanning calorimetry (DSC). Micelles of these materials were prepared in a selective solvent for the poly(isoprene) blocks. The radius of the micelles and the radius of the core were obtained experimentally by DLS and atomic force microscopy (AFM), respectively. Finally, the results were compared to theoretical scaling predictions for block copolymer micelles.

Experimental Section

Reagents and Solvents. All solvents and monomers for the synthesis of the block copolymers were distilled after the corresponding drying procedure and stored under argon. Cyclohexane (Biosolve) was distilled from polystyryllithium oligomers. 1,1-Diphenylethylene (Aldrich) was dried over *sec*-butyllithium and distilled under vacuum. Styrene (Aldrich) was refluxed over calcium hydride (Aldrich) for 24 h, distilled under reduced pressure, and stored under argon and over a sodium mirror at −25 °C. Isoprene (Aldrich) was purified in the same way as styrene but distilled at atmospheric pressure. *sec*-Butyllithium (1.4 M) in cyclohexane (Aldrich) was used as received. All other solvents and reagents were used as received. Methanol (Biosolve) was degassed with argon for 15 min just prior to use.

Diblock Copolymer Synthesis and Characterization. Sequential anionic polymerizations for the synthesis of poly((styrene-*alt*-diphenylethylene)-*b*-isoprene) (P(S-*alt*-DPE)-*b*-PI) were performed in a Chemspeed ASW2000 synthesizer, comprising up to 20 glass reactors of 75 mL or 80 glass reactors of 13 mL equipped with heating/cooling jacket, a glovebox for inert atmosphere, a vortex stirring system (0−1400 rpm), a heating/cooling system (−90 to 150 °C), and a fully automated liquid handling system. The use of this synthesizer ensures that all experiments were performed under the same reaction conditions (atmosphere, same experimental error, etc.), and therefore the obtained results are easily comparable and reproducible.[25] In a typical procedure (Scheme 1) the anionic synthesis of the block copolymers was performed as follows: a predetermined amount of 1,1-diphenylethylene was added into the reactors of the synthesizer containing a predetermined amount of cyclohexane at 50 °C and 450 rpm of vortexing under an argon atmosphere. Addition of *sec*-butyllithium into the reactors transformed the 1,1-diphenylethylene to the corresponding 1,1-diphenylalkyllithium, resulting in the characteristic red color. After 0.5 h, an equimolar quantity of styrene (with respect to 1,1-diphenylethylene) was introduced into the reaction media and reacted for 2 h. Thereafter, samples were withdrawn from the reaction media for GPC characterization of the poly(styrene-*alt*-1,1-diphenylethylene) block (P(S-*alt*-DPE)). Addition of a predetermined volume of isoprene into the reactor initiated the polymerization of the second block. After 4 h of reaction at room temperature the reaction was terminated by addition of methanol. Purification of the polymers was performed with two cycles of dissolution/precipitation (chloroform/methanol). The obtained block copolymers were dried at 40 °C under vacuum for 24 h and were subsequently characterized by GPC, ^{1}H NMR, and DSC in order to obtain the molecular weights, the compositions of each block, and glass transition temperatures, respectively.

Micelle Preparation and Characterization. Micelle preparation from the synthesized block copolymers was performed using methods reported in the literature.[8] Bulk block copolymers were dissolved in a common solvent (chloroform, good solvent for both blocks) (1 g/L) at room temperature. Subsequently, a selective precipitant for the styrenic block (*n*-heptane) was gradually added to reach a concentration of 10 wt % of the common solvent (chloroform). The removal of chloroform from the mixtures was achieved by heating the solutions at 60 °C in an oil bath for 1 h. The resulting block copolymer micellar solutions were finally diluted with an excess of *n*-heptane (up to 10-fold excess). These solutions were characterized subsequently by DLS (in *n*-heptane) and AFM (dry conditions) in order to determine the hydrodynamic diameter and the diameter of the core of the accordingly formed micelles. It was found that some of the micellar solutions were unstable in time (especially sample **2** in Table 1). DLS measurements revealed that when using not freshly prepared micellar solutions bimodal distributions are obtained, suggesting the collapse or aggregation of the micelles. Therefore, the herein reported DLS measurements were recorded on freshly prepared micellar solutions, and additionally, the solutions were filtered two times on 200 nm syringe filters immediately after the removal of chloroform in order to avoid the formation of micellar aggregates.

Characterization Techniques. GPC measurements were performed on a Shimadzu system with a SCL-10A system controller, a LC-10AD pump, a RID-6A refractive index detector, and a Polymer Laboratories Plgel 5 μm Mixed-D column. A solution of 4% triethylamine and 2% 2-propanol in chloroform was used as an eluent at a flow rate of 1 mL/min. Molecular weights were calculated against polystyrene standards.

^{1}H NMR spectra were recorded at room temperature on a Varian Gemini 400 spectrometer using deuterated chloroform (Cambridge Isotopes Laboratories). The 1,4-unit content of PI was calculated from the relative intensity of the signal at 5.1 ppm (−CH= of 1,4-unit) and the signals at 4.68 and 4.75 ppm (=CH$_2$ of 3,4-unit and =CH$_2$ of 1,2-unit). The copolymer composition was calculated from the relative intensities of the

Table 1. Characteristics of the Synthesized Poly((styrene-*alt*-1,1-diphenylethylene)-*b*-isoprene) (P(S-*alt*-DPE)-*b*-PI) Block Copolymers

	M_n/PDI (GPC) P(S-*alt*-DPE)	M_n/PDI (GPC) P(S-*alt*-DPE)-*b*-PI	mol % (^{1}H NMR) PI	microstructure (^{1}H NMR) 1,4-unit % PI	T_{g1} (°C)	T_{g2} (°C)
1	7600/1.18	22000/1.10	71	89	−50	175
2	6100/1.20	33200/1.09	83	90	−52	185
3	12700/1.19	27900/1.24	60	90	−47	185
4	8500/1.36	53300/1.11	85	88	−50	179

signals for the 1,4-unit, 1,2-unit, and 3,4-unit of PI block and from the *meta* and *para* hydrogens of the aromatic rings at 6.93 ppm of the P(S-*alt*-DPE) block.

Differential scanning calorimetry (DSC) was performed on a Netzsch DSC 204 F1 instrument calibrated with indium. Multiple heating and cooling scans were generated over a temperature range of −150 to 230 °C using a scan rate of 20 and 40 °C/min with nitrogen as the purge gas. The glass transition temperatures were noted at the inflection points of the heat capacity jump.

DLS experiments were performed at 25 °C at 90° on a Malvern CGS-3 apparatus equipped with a 633 nm laser. The used values of the refractive index and viscosity of *n*-heptane were 1.385 and 3.94 Pa·s, respectively.

For the AFM experiments, samples were prepared by spin-casting of 100-fold diluted micellar solutions (in order to obtain near monolayer coverage) onto freshly cleaved mica substrates. The samples were prepared and imaged within 30 min to reduce the possibility of micelle deformation and/or aggregation. Imaging was performed in intermittent contact mode on a Multimode SPM (Digital Instruments, Santa Barbara, CA) using NSC36-type tips (~1 N/m, Mikromasch, Spain). The height of the micelles was determined from histograms after zeroth-order leveling of the images.

Results and Discussion

As mentioned in the Experimental Section, the synthesis of the diblock copolymers was performed by sequential anionic polymerization. This synthetic approach is depicted in Scheme 1, and the characteristics of the polymers are summarized in Table 1. Figures 1, 2a, and 3 show the GPC traces, ^{1}H NMR spectra, and DSC traces of one of the synthesized materials (**1**, Table 1). The other block copolymers revealed similar characteristics to those displayed in Figures 1, 2a, and 3.

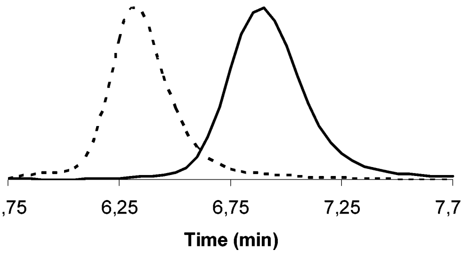

Figure 1. Typical GPC traces for the P(S-*alt*-DPE) precursor (solid trace) and the P(S-*alt*-DPE)-*b*-PI diblock copolymer (dashed trace) of sample **1** (Table 1).

Figure 1 shows GPC traces indicating the successful chain extension of the polymer and single narrow molecular weight distributions for the P(S-*alt*-DPE) precursor as well as the P(S-*alt*-DPE)-*b*-PI diblock copolymer. The polydispersity indices (PDI) of the synthesized materials listed in Table 1 reveal that the molecular weight distributions of the precursor blocks are slightly broader than those of the corresponding P(S-*alt*-DPE)-*b*-PI diblock copolymers. This effect has been very frequently reported in the literature.[23]

Figure 2 shows the differences in the ^{1}H NMR spectra for one of the synthesized P(S-*alt*-DPE)-*b*-PI diblock copolymers (A) and one "regular" PS-*b*-PI diblock copolymer (B) synthesized and characterized in similar conditions. The main difference between the ^{1}H NMR spectra of Figure 2 arises in the aromatic region. In this region it can be seen that the incorporation of extra phenyl rings in the styrenic block (copolymerization with 1,1-diphenylethylene) shifts the aromatic signals to lower fields and leads to broader peaks and the appearance of a new signal at 5.93 ppm. The microstructure of the PI block was investigated by ^{1}H NMR, revealing a content of 1,4-units of around 89% for all the samples (Table 1). The M_n of the PI block was calculated from the copolymer composition as determined by ^{1}H NMR and from the molecular weight of the respective diblock copolymers as determined by GPC. An alternative method to obtain the M_n of the PI block and the copolymer composition is from the difference between the molecular weights of the P(S-*alt*-DPE)-*b*-PI diblock copolymer and the P(S-*alt*-DPE) copolymer as obtained by GPC. These latter calculations were in agreement to those found using the ^{1}H NMR approach.

DSC is a suitable technique to detect phase separation in block copolymers with immiscible polymeric components when the individual glass transition temperatures (T_g) are sufficiently different from each other, and the copolymer composition is far enough from the extreme values. A typical DSC trace obtained for one of the diblock copolymers of this study (**1**, Table 1) is shown in Figure 3. One main transition is clearly observed around −50 °C corresponding to the PI block, whereas

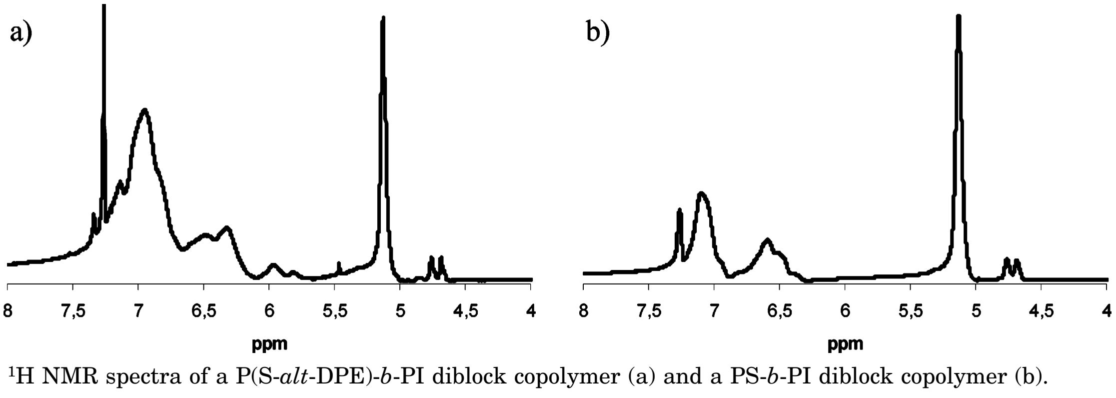

Figure 2. ^{1}H NMR spectra of a P(S-*alt*-DPE)-*b*-PI diblock copolymer (a) and a PS-*b*-PI diblock copolymer (b).

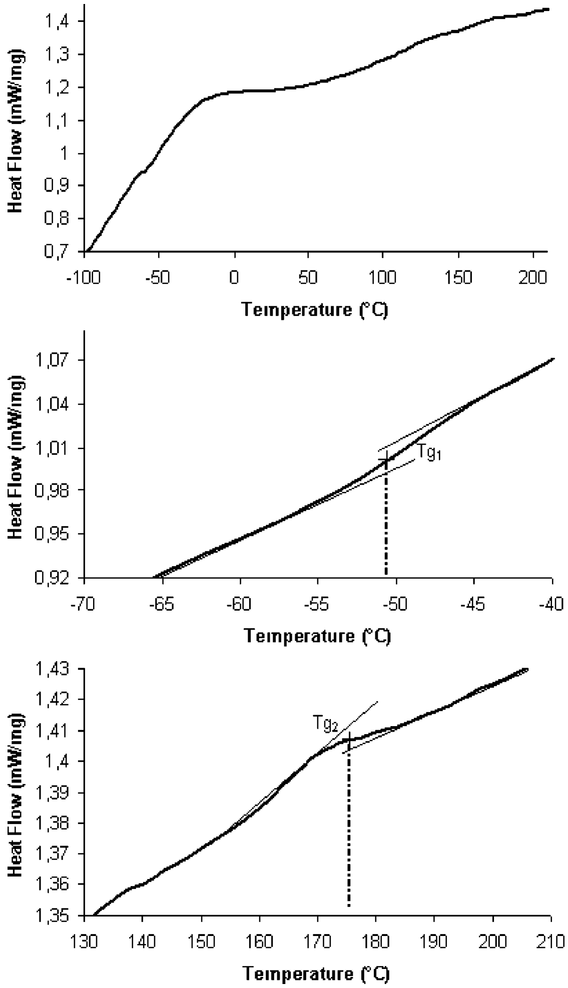

Figure 3. DSC trace recorded at a heating rate of 20 °C/min for sample **1** (Table 1).

a small transition could be detected around 175 °C which is related to the P(S-*alt*-DPE) block. It is known that the microstructure of polydienes and polymers in general has a strong influence on the T_g of materials.[26] For all materials analyzed in this work the diblock copolymers presented a content of 89% of 1,4-units and a T_g around −50 °C for the PI block, as summarized in Table 1 (T_{g1}). The T_g corresponding to the P(S-*alt*-DPE) blocks is mainly ruled by the content of 1,1-diphenylethylene as reported in the literature (T_g increases by 1.26 °C/wt % of 1,1-diphenylethylene in the copolymer).[23] For the present diblock copolymers the wt % of 1,1-diphenylethylene within the P(S-*alt*-DPE) block is 63.3% (highest possible content, corresponding to a ratio of 50% mol of styrene and 50% mol of 1,1-diphenylethylene) in which case the T_g must be around 180 °C. Table 1 shows that the experimental T_g values of the P(S-*alt*-DPE) block (T_{g2}) are in agreement with the values reported in the literature.

Regarding the study of diblock copolymer micelles, control over the micellar size can be obtained by varying the block copolymer composition and/or degree of polymerization. Scaling theories for micelles of linear AB-type block copolymers with an insoluble B-block have been examined for two extreme cases.[8,12,27] Micelles in which the degree of polymerization for the insoluble block (N_B) is much smaller than the soluble block (N_A) are called “hairy” micelles while systems in which N_A is smaller than N_B are called “crew-cut” micelles (Figure 4).

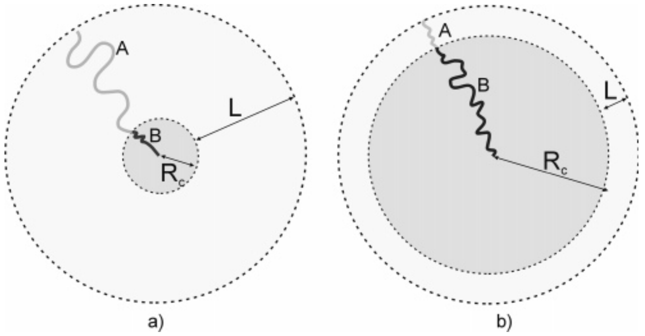

Figure 4. Schematic depictions of (a) a “hairy” micelle and (b) a “crew-cut” micelles composed of linear diblock copolymers with a soluble A-block and insoluble B-block.

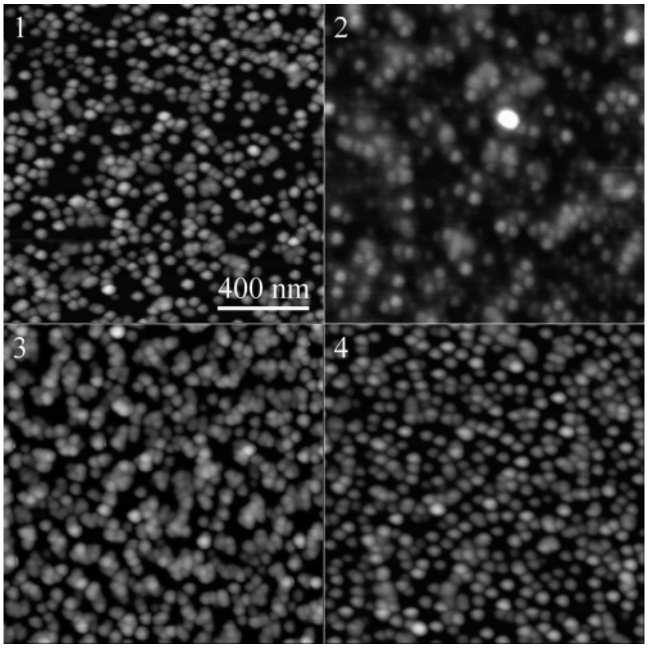

Figure 5. Intermittent contact mode height images of P(S-*alt*-DPE)-*b*-PI micelles. The number in the corner indicates different block copolymer compositions according to samples of Tables 1 and 2. Lateral dimensions and the *z* range are 1 × 1 μm² and 25 nm for all images.

Assuming uniformly stretched chains for the core, the radius of the core (R_C) and the aggregation number (Z) for “crew-cut”-type micelles can be predicted by

$$R_C \propto \gamma N_B^{2/3} a \qquad Z \propto \gamma N_B \tag{1}$$

where γ is the A/B interfacial tension and a the segment length.[8,15]

In the case of “hairy” micelles (with $N_A > N_B^{4/5}$) in a good solvent, the radius of the core (R_C), the aggregation number (Z), and the thickness of the corona (L) scale by the equations listed under eq 2. The radius of the complete micelle ($R = R_C + L$) is dominated by the degree of polymerization of block A. This demonstrates that for “hairy” micelles the diameter is dominated by the thickness of the corona.

$$Z \propto N_B^{4/5} \qquad R_C \propto N_B^{3/5} a \qquad L \propto N_A^{3/5} N_B^{6/25} a \tag{2}$$

n-Heptane acts as a good solvent for the PI block and a bad solvent for the P(S-*alt*-DPE) block, resulting in the formation of micelles in which the core is comprised of P(S-*alt*-DPE) copolymers and the corona is consisting

Table 2. Size of the Micelles Determined by AFM and DLS[a]

	M_n (GPC) P(S-*alt*-DPE)-*b*-PI	N_B (core)	N_A (corona)	R_C (nm) (AFM)	R (nm) (DLS)	L (nm) ($R - R_C$)
1	22 000	54	228	5.0	30	25.0
2	33 200	43	405	4.0	38	34.0
3	27 900	89	246	7.7	40	32.3
4	53 300	60	665	5.6	52	46.4

[a] Diameter of the core of the micelles was estimated from the observed height in AFM. The entire micelle diameter (nm) in *n*-heptane was obtained by DLS. N_B refers to the degree of polymerization of the P(S-*alt*-DPE) block (insoluble block) and N_A to the degree of polymerization of the PI block (soluble block).

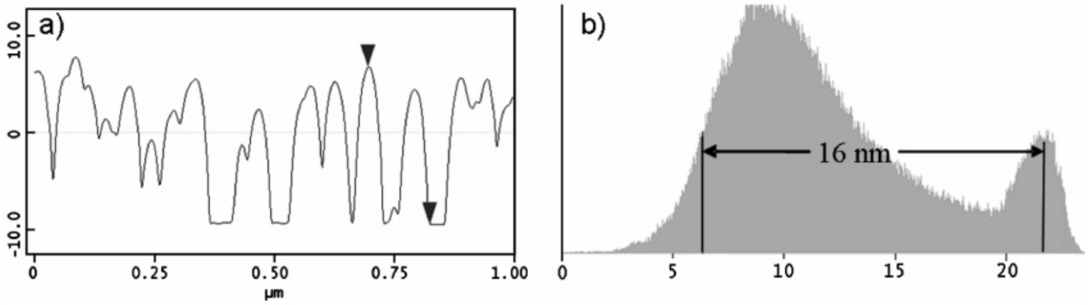

Figure 6. Height of the micelles can be determined in two ways. (a) The height can be obtained by averaging the results from cross sections. (b) The distance between the surface peak and the bending point of the particle peak corresponds to the average micelle height. See Supporting Information for details and a schematic description.

of extended PI chains. The degree of polymerization of the P(S-*alt*-DPE) blocks (N_B) was determined from GPC data using the average of the molecular weights of styrene and 1,1-diphenylethylene (142.2 g/mol), whereas the degree of polymerization of the PI block (N_A) was calculated from ^{1}H NMR and GPC data of the diblock copolymers and the molecular weight of isoprene (68.12 g/mol). According to the information in Tables 1 and 2, hairy-type micelles are expected for all experiments since N_A is larger than $N_B^{4/5}$. The hydrodynamic diameter of the micelles was evaluated by DLS whereas the diameter of the core was obtained from AFM. When compared to the known poly(styrene-*b*-isoprene) block copolymer micelles,[19] P(S-*alt*-DPE) is a relatively harder, stiffer block. This should lead to a decreased critical micelle concentration.[28] Because AFM measurements were performed at room temperature (well below the glass transition temperature of the P(S-*alt*-DPE) core of the micelles), the core is expected to be thermodynamically frozen[20] and stable during AFM imaging at dry conditions. Figure 5 displays the observed intermittent contact mode height images of the dried micelles. From the images it can be confirmed that all micelles are spherical and have a narrow distribution. To avoid tip convolution effects, the diameter of the micelles was estimated by measuring the observed height of the micelles. Because micelles typically have a Gaussian size distribution, accurate determination of their height requires reliable averaging techniques. The average height of the micelles was determined for each polymer composition by two methods (see Figure 6 for an example (sample **3**, Table 1)). In the first method, the average micellar height is determined by evaluating many cross sections (Figure 6a). The second method involves the evaluation of histograms for each image. The histogram in Figure 6b depicts the relative abundance of heights. For a sample consisting of flat particles on a flat substrate two peaks should appear with the distance between them representing the difference in height between the particles and the background. For the micelles the histogram reveals the presence of two broadened peaks. The peak at low height indicates the level of the mica substrate whereas the other peak indicates the presence of particles on the surface.[29] By evaluating many histograms, it was found that the distance between the center of the "mica peak" and the bending point of the "particle peak" corresponds to the average height of the particles determined by the cross-section method (see Supporting Information). It is advantageous to determine the height by this method because it is highly reproducible and in addition it significantly reduces the required analysis time. This latter method has been confirmed independently using gold nanoparticles with known height (see Supporting Information). The sizes of the cores of the prepared micelles (samples of Table 1) found by AFM are summarized in Table 2. In contrast to other experimental techniques (such as TEM) to determine size of the core of micelles, AFM imaging does not require staining or UHV conditions and reduces the possibility of the core deformation.

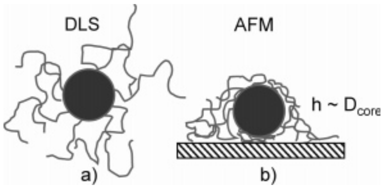

Figure 7. Schematic depictions of the diblock copolymer micelle architecture during the characterization by (a) DLS (hydrodynamic diameter of the entire micelle in solution) and (b) AFM (diameter of the core of the micelle, height).

From the height images in Figure 5 one can already observe that micelles prepared from sample **2** (containing a small fraction of core blocks) are not so well-defined. The micellar heights (~8 nm) for this sample are more broadly distributed. DLS measurements also showed that micelles prepared from sample **2** were rather unstable. This observation can be explained by looking at the polymer composition (Table 1). The P(S-*alt*-DPE) block of sample **2** is the shortest one ($N_B \sim 43$). Obviously, the low degree of polymerization may be the origin of the decreased micellar stability.

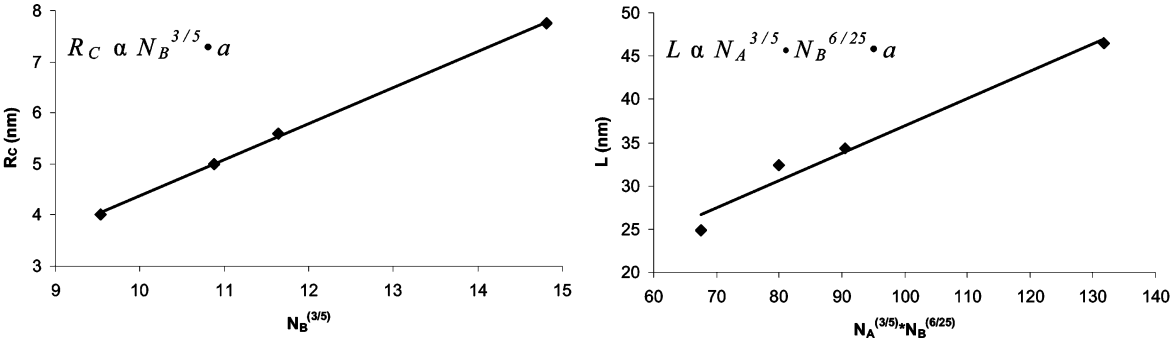

Figure 8. (left) Radius of the micelle core (R_C) obtained by AFM has been plotted as a function of the degree of polymerization of the insoluble block (N_B) (eq 2). Square dots represent actual data points whereas a linear fit ($R = 0.999$) is plotted as a guide to the eye. (right) Thickness of the corona ($L = R - R_C$) obtained from data of DLS and AFM has been plotted as a function of the degree of polymerization of the soluble and insoluble blocks (N_A, N_B) (eq 2). Square dots represent actual data points whereas a linear fit ($R = 0.977$) is plotted as a guide to the eye. See Table 2 for details and numerical values.

Table 3. Obtained Values of Monomer Size or Segment Length *a* of Each Block of the Studied Micelles (Calculations Were Performed Using Eq 2 and Data Presented in Figure 5)[a]

	1	2	3	4
a_C (core) (nm)	0.46	0.42	0.52	0.48
a_L (corona) (nm)	0.37	0.38	0.40	0.35

[a] a_C = segment length of the core (P(S-*alt*-DPE) block). a_L = segment length of the shell (PI block).

DLS was used to study the micellar size in solution using the Cumulants analysis method.[30] Table 2 summarizes the hydrodynamic radius of the micelles obtained by DLS (R), the radius of the core obtained by AFM (R_C), and the thickness of the corona (L). The thickness of the corona compared to the size of the core confirms that the micelles are all of the "hairy" type. At first sight the radii of the micelles obtained by AFM and DLS do not correlate to the molecular weight, even their relative order is different: by AFM the largest observed micelles are made from polymer **3**, whereas DLS indicates polymer **4**. This discrepancy is explained because the radius obtained by DLS is the hydrodynamic one whereas the AFM is used to determine the height of micelles adsorbed on a flat surface. The hydrodynamic diameter is, in the case of "hairy" micelles, dominated by the degree of polymerization of the soluble polyisoprene block (eq 2). For AFM images on dried micelles, the corona is no longer swollen by the solvent. The flexible coronal chains are expected to be oriented flat on the surface, and therefore the height of the micelles essentially corresponds the size of the core (Figure 7).

Indeed, it is found that the height of the micelles correlates very well to the degree of polymerization of the core block (P(S-*alt*-DPE)) (Figure 8). According to theory,[8] the diameter of the micelle and the core can be estimated from the degree of polymerization of both blocks. In Figure 8, the radius of the core (R_C) and the thickness of the corona (L) have been plotted against $N_B^{3/5}$ and $N_A^{3/5}N_B^{6/25}$, respectively. Both plots clearly demonstrate a linear correlation indicating the validity of the theoretical model as well as the applicability of using AFM imaging to micelles in the dried state to determine the diameter of the core. Moreover, estimation of the proportionality constants for the equations of R_C and L (eq 2) can be performed using the data presented in Figure 8. These proportionality constants may be the equivalent to the monomer size or segment length a in eq 2 of the corresponding block or section of the micelles. Table 3 summarizes these calculations for the segment length of the core (a_C) and for the segment length of the corona (a_L) of each of the studied micelles. From Table 3 it can be seen that the obtained values for the different segment lengths of the cores (a_C) have a tendency to be constant with an average value of 0.47 nm and standard deviation of 0.04. The average value of 4.7 Å is a reasonable value for an organic molecule and may correspond to the average molecular size of the involved monomeric units (styrene and 1,1-diphenylethylene). The obtained values for the different segment lengths of the coronas (a_L) revealed an average value of 0.38 nm and standard deviation of 0.02, which is also a reasonable value for the size of the isoprene monomer. It should be noted that experimental factors related with the DLS measurements and the determination of the degree of polymerization of the PI block can influence the modeling of the thickness of the corona.

Conclusion

In this contribution the synthesis of "new" diblock copolymers of the type of poly((styrene-*alt*-diphenylethylene)-*b*-isoprene) via sequential anionic polymerization as well as their characterization is presented. Modified 1,1-diphenylethylene commodity elastomers have appeared recently as an alternative for high-temperature applications. The main advantage of these materials over the well-known elastomers is the enhancement of their properties at these conditions. The obtained materials were utilized for the preparation of polymeric micelles using a selective solvent for one of the blocks. The hydrodynamic radius of the micelles was determined by DLS whereas the size of the micellar core was obtained from AFM measurements at dry conditions. Theory states that the core size, corona thickness, and micellar diameter depend on the degree of polymerization of both blocks. For so-called "hairy" micelles the diameter of the whole micelle in solution is dominated by the thickness of the corona. It was found that the observed characteristics of the studied micelles correlate to the theoretical scaling predictions. Moreover, the average size of the monomeric units could be determined with high precision from the obtained experimental data and the theoretical knowledge.

Acknowledgment. The authors thank the Dutch Polymer Institute and NWO for financial support. C.A.F. is "Chargé de Recherches" by the FNRS. J.F.G. thanks the FNRS for financial support (DLS equipment).

Supporting Information Available: Explanation and validation of the determination of the average height of spherical particles using the histogram method. This material is available free of charge via the Internet at http://pubs.acs.org.

References and Notes

(1) (a) Liu, S. Q.; Tong, Y. W.; Yang, Y.-Y. *Biomaterials* **2005**, *26*, 5064−5074. (b) Zeng, F.; Liku, J.; Allen, C. *Biomacromolecules* **2004**, *5*, 1810−1817. (c) Savic, R.; Luo, L.; Eisenberg, A.; Maysinger, D. *Science* **2003**, *300*, 3465−3484. (d) Kakizawa, Y.; Kataoka, K. *Adv. Drug. Del. Rev.* **2002**, *54*, 191−202.

(2) (a) Li, X.; King, H. A.; Kim, D. H.; Knoll, W. *Langmuir* **2005**, *21*, 5212−5217. (b) Kang, Y.; Taton, T. A. *Angew. Chem., Int. Ed.* **2005**, *44*, 409−412. (c) Spatz, J. P.; Moessmer, S.; Hartmann, C.; Moeller, M. *Langmuir* **2000**, *16*, 407−415. (d) Cuenya, B. R.; Baeck, S. H.; Jaramillo, T. F.; McFarland, E. W. *J. Am. Chem. Soc.* **2003**, *125*, 12929−12934. (e) Kaestle, G.; Boyen, H.-G.; Weigl, F.; Lengl, G.; Herzog, T.; Ziemann, P.; Riethmueller, S.; Mayer, O.; Hartmann, C.; Spatz, J. P.; Moeller, M.; Ozawa, M.; Banhart, F.; Garnier, M. G.; Oelhafen, P. *Adv. Funct. Mater.* **2003**, *13*, 853−861.

(3) Pedersen, J. S.; Hamley, I. W.; Ryu, C. Y.; Lodge, T. P. *Macromolecules* **2000**, *33*, 542−550.

(4) Minatti, E.; Borsali, R.; Schappacher, M.; Deffieux, A.; Soldi, V.; Narayanan, T.; Putaux, J.-L. *Macromol. Rapid Commun.* **2002**, *23*, 978−982.

(5) Svensson, M.; Alexandridris, P.; Linse, P. *Macromolecules* **1999**, *32*, 637−645.

(6) (a) Yang, L.; Alexandridis, P. *Curr. Opin. Colloid Interface Sci.* **2000**, *5*, 132−143. (b) Discher, D. E.; Eisenberg, A. *Science* **2002**, *297*, 967−973. (c) Discher, B. M.; Won, Y. Y.; Ege, D. S.; J. Lee, C.-M.; Bates, F. S.; Discher, D. E.; Hammer, D. A. *Science* **1999**, *284*, 1143−1146.

(7) (a) Yu, K.; Eisenberg, A. *Macromolecules* **1998**, *31*, 3509−3518. (b) Yu, K.; Zhang, L.; Eisenberg, A. *Langmuir* **1996**, *12*, 5980−5984. (c) Yu, K.; Bartels, C.; Eisenberg, A. *Langmuir* **1999**, *15*, 7157−7167. (d) Yu, K.; Eisenberg, A. *Macromolecules* **1998**, *31*, 3509−3518.

(8) Riess, G. *Prog. Polym. Sci.* **2003**, *28*, 1107−1170.

(9) (a) Mortensen, K. Small angle scattering studies of block copolymer micelles, micellar mesophases and networks. In *Amphiphilic Block Copolymers: Self-Assembly and Applications;* Alexandridis, P., Lindman, B., Eds.; Elsevier: Amsterdam, 2000; pp 191−220. (b) Munk, P. Classical methods for the study of block copolymer micelles. In *Solvents and Self-Organization of Polymer;* Webber, S. E., Munk, P., Tuzar, Z., Eds.; NATO ASI Series E: Applied Sciences; Kluwer Academic Publisher: Dordrecht, 1996; Vol. 327, pp 367−381.

(10) Hamley, I. W. *The Physics of Block Copolymers*; Oxford Science Publication: Oxford, 1998.

(11) Linse, P. Modelling of self-assembly of block copolymers in selective solvents. In *Amphiphilic Block Copolymers: Self-Assembly and Applications;* Alexandridis, P., Lindman, B., Eds.; Elsevier: Amsterdam, 2000; pp 13−40.

(12) Shusharina, N. P.; Linse, P.; Khokhlov, A. R. *Macromolecules* **2000**, *33*, 3892−3901.

(13) Milchev, A.; Bhattacharya, A.; Binder, K. *Macromolecules* **2001**, *34*, 1881−1893.

(14) (a) Noolandi, R.; Hong, K. M. *Macromolecules* **1983**, *16*, 1433−1448. (b) Nagarajan, R.; Ganesh, K. *Macromolecules* **1989**, *22*, 4312−4325.

(15) (a) Halperin, A.; Alexander, S. *Macromolecules* **1989**, *22*, 2403−2412. (b) Halperin, A. *Macromolecules* **1987**, *20*, 2943−2949.

(16) Vangeyte, P.; Leyh, B.; Heinrich, M.; Grandjean, J.; Bourgaux, C.; Jérôme, R. *Langmuir* **2004**, *20*, 8442−8451.

(17) Pitsikalis, M.; Siakali-Kioulafa, E.; Hadjichristidis, N. *J. Polym. Sci., Part A: Polym. Chem.* **2004**, *42*, 4177−4188.

(18) (a) Inoue, T.; Soen, T.; Hashimoto, T.; Kawai, H. *J. Polym. Sci., Part A-2* **1969**, *7*, 1283−1302. (b) Girolamo, M.; Urwin, J. R. *Eur. Polym. J.* **1971**, *7*, 225−230. (c) Busch, P.; Posselt, D.; Smilgies, D.; Rheinländer, B.; Kremer, F.; Papadakis, C. M. *Macromolecules* **2003**, *36*, 8717−8727.

(19) (a) Wilson, D. J.; Riess, G. *Eur. Polym. J.* **1988**, *24*, 617−621. (b) Pispas, S.; Hadjichristidis, N.; Potemkim, I.; Khokhlov, A. *Macromolcules* **2000**, *33*, 1741−1746. (c) Sotiriou, K.; Nannou, A.; Velis, G.; Pispas, S. *Macromolcules* **2002**, *35*, 4106−4112. (d) Zhu, F.; Ngai, T.; Xie, Z.; Wu, C. *Macromolecules* **2003**, *36*, 7405−7408. (e) Ouarti, N.; Viville, P.; Lazzaroni, R.; Minatti, E.; Schappacher, M.; Deffieux, A.; Borsali, R. *Langmuir* **2005**, *21*, 1180−1186. (f) Mountrichas, G.; Mpiri, M.; Pispas, S. *Macromolecules* **2005**, *38*, 940−947.

(20) Spěváček, J. *Makromol. Chem., Rapid Commun.* **1982**, *3*, 697−703.

(21) Trepka, W. J. *Polym. Lett.* **1970**, *8*, 499−503.

(22) Scheirs, J.; Priddy, D. *Modern Styrenic Polymers*; Wiley: West Sussex, 2003; pp 581−603.

(23) Xu, J. J.; Bates, F. S. *Macromolecules* **2003**, *36*, 5432−5434.

(24) (a) Yuki, H.; Kosai, K.; Murahashi, S.; Hotta, J. *Polym. Lett.* **1964**, *2*, 1121−1125. (b) Hsieh, H. L.; Quirk, R. P. *Anionic Polymerization: Principles and Practical Applications;* Marcel Dekker: New York, 1996. (c) Quirk, R. P.; Yoo, T.; Lee, Y.; Kim, J.; Lee, B. *Adv. Polym. Sci.* **2000**, *153*, 96−101.

(25) Guerrero-Sanchez, C.; Abeln, C. H.; Schubert, U. S. *J. Polym. Sci., Part A: Polym. Chem.* **2005**, *43*, 4151−4160.

(26) Yu, J. M. Dubois, P.; Teyssié, P.; Jérôme, R. *Macromolecules* **1996**, *29*, 6090−6099.

(27) (a) Gast, A. P. *Solvents and Self-Organization of Polymers;* NATO ASI Series E: Applied Sciences; Kluwer Academic Publisher: Dordrecht, 1996; Vol. 327, pp 259−280. (b) van der Burgh, S.; de Keizer, A.; Cohen Stuart, M. A. *Langmuir* **2004**, *20*, 1073−1084.

(28) Klok, H. A.; Lecommandoux, S. *Adv. Mater.* **2001**, *13*, 1217−1229.

(29) A histogram of a flat surface with flat particles would have two peaks with the distance between the two peaks equal to the particle height. A surface with spherical particles shows a tailing peak because the highest point of the spheres is less abundant. Therefore, the distance between the peak maxima does not correspond to the sphere height (Supporting Information).

(30) Brown, W. *Dynamic Light Scattering*; Oxford University Press: Oxford, 1972.

MA051544U